Contrib. Astron. Obs. Skalnaté Pleso **43**, 229 – 236, (2014)

Speckle Interferometry

R. Köhler

Max-Planck-Institut für Astronomie, Königstuhl 17, 69117 Heidelberg, Germany, (E-mail: koehler@mpia.de)

Received: November 1, 2013; Accepted: January 8, 2014

Abstract. Speckle interferometry has proven to be a powerful method for high-angular-resolution observations. With relatively little instrumental effort, it is possible to resolve structures at the diffraction limit of the telescope and measure, e. g., binary parameters. This makes it an ideal method for projects like orbital monitoring of binary systems with periods of more than a few years. However, due to the complex methods required to reduce the data, not very many astronomers know how to use it.

I describe the basic methods used to reconstruct modulus and phase of the Fourier-transformed high-resolution image from speckle data. I also show some example data of binary stars, and demonstrate why the simple structure of the Fourier transform of binary star images makes them ideal targets for speckle interferometry. Finally, I present some of the results that were obtained using speckle interferometry.

Key words: instrumentation: high angular resolution – methods: data analysis – techniques: high angular resolution

1. Introduction

Many astronomical applications require observations with high spatial resolution. However, direct imaging with ground-based telescopes is limited by the turbulence of the atmosphere, which blurs the images of point sources to a broad peak with a diameter of the order of $1''$ (see Fig. 1, left panel), so all high-resolution information is lost.

Fortunately, with sufficiently short integration times, the turbulent atmosphere is "frozen", so we can obtain images that retain the high-resolution information. Sufficiently short means about as long as the coherence time of the atmosphere, which is of the order of about 60 milliseconds in the near-infrared (Leinert 1994). The middle panel of Fig. 1 shows an example. The image is still distorted by the inhomogeneous atmosphere, which causes the characteristic specks of light that gave the method its name. (It is called speckle *interferometry* because the short-exposure images are interferograms of the atmosphere.) The signal-to-noise ratio of these images is very poor, so that detection of even moderately faint companions is difficult or impossible.

The way to overcome this problem is to take many images, usually several hundred or thousand, and combine them in a way that preserves the small structures.

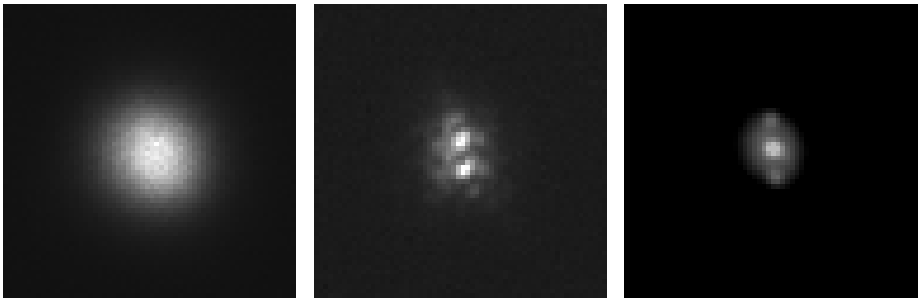

Figure 1. *Left:* A long (125 sec) exposure of the star RX J1602.9-2022. *Middle:* The same star in an image exposed for only 0.5 sec. *Right:* An image of the star obtained with the shift-and-add method, using about 125 input images. The field-of-view of the images is 3″, and the separation of the binary is 0.31″.

2. Lucky Imaging and Shift-and-Add

The middle panel in Fig. 1 shows that once in a while, a short-exposure image happens to contain an almost undistorted representation of the astronomical target. If we collect enough individual images, a certain percentage of them will be such lucky cases. By selecting only the sharpest images and adding them up, we can obtain an image with much higher resolution than a long exposure. This method is called "lucky imaging". The percentage of images that can be used depends on the atmospheric turbulence during the observation. It is usually in the range between 1 % and a few times 10 %. Therefore, most of the recorded data have to be thrown away.

A method that is often combined with lucky imaging is the so-called shift-and-add method. It can also be applied without selecting the sharpest images beforehand, in particular with observations in the infrared. For shift-and-add, one searches for the brightest pixel in each image, shifts the image so that this pixel is in the center, and then adds the shifted images together. An example for the result is shown in the right-hand panel of Fig. 1. There are two major disadvantages when using this method for binary stars: First, if the two components have similar brightness, the brightest pixel is not always on the primary. Shift-and-add images of these systems look like a triple star with three components on a straight line. Second, only the brightest speckle contributes to the central peak, the rest of the light creates a halo around the star. Both effects make it impossible to obtain useful photometric information from shift-and-add images of close binaries. Other implementations are possible, e.g. use the center of light instead of the brightest pixel, but the problem of the halo remains.

3. Powerspectrum Analysis

In order to understand the way speckle interferometry overcomes these limitations, we have to examine what happens to the light on the way to the telescope. The image $I(x)$ we record on our detector is the convolution of the true brightness distribution of the object $O(x)$ with the so-called point spread function (PSF) $P(x)$:

$$I(x) = \int O(x') \cdot P(x - x') \, \mathrm{d}x' \, .$$

(Note that x and x' are positions in the two-dimensional image plane). A Fourier-transform turns the convolution into a product:

$$\tilde{I}(u) = \tilde{O}(u) \cdot \tilde{P}(u) \, .$$

The simple idea to divide $\tilde{I}(u)$ by $\tilde{P}(u)$ to get $\tilde{O}(u)$ is not feasible because $\tilde{P}(u)$ may contain zeroes, $\tilde{I}(u)$ is noisy, and because we usually do not know $\tilde{P}(u)$.

Labeyrie (1970) proposed to use the power spectrum of the image $|\tilde{I}(u)|^2$ and average the power spectra of many images. This quantity is much less problematic with regard to zeroes and noise, and it varies much slower over time. Thus, we can observe an unresolved star[1] shortly before or after the science target. Since the brightness distribution of an unresolved star is a delta-function, an image of it is simply the PSF:

$$I_{\mathrm{ref}}(x) = \int \delta(x') \cdot P(x - x') \, \mathrm{d}x' = P(x) \, .$$

From the power spectra of the images of the science object and the reference star we obtain the power spectrum of the brightness distribution of the science target:

$$|\tilde{O}(u)|^2 = \frac{< |\tilde{I}_{\mathrm{obj}}(u)|^2 >}{< |\tilde{I}_{\mathrm{ref}}(u)|^2 >} \, ,$$

where $< \ldots >$ denotes averaging over several images.

The Fourier-transform of the brightness distribution $\tilde{O}(u)$ is called the complex visibility. From the power spectrum, we can obtain only its modulus $|\tilde{O}(u)|$, which is usually called the visibility. However, the modulus contains almost every piece of information we want to know about a binary. One can see in the examples in Fig. 2 that the direction of the stripe pattern gives us the position angle of the binary, the distance of the stripes is inversely proportional to the binary separation, and the contrast of the stripes gives the flux ratio of the components.

[1] Finding such a star is not trivial, of course, since many stars are binaries.

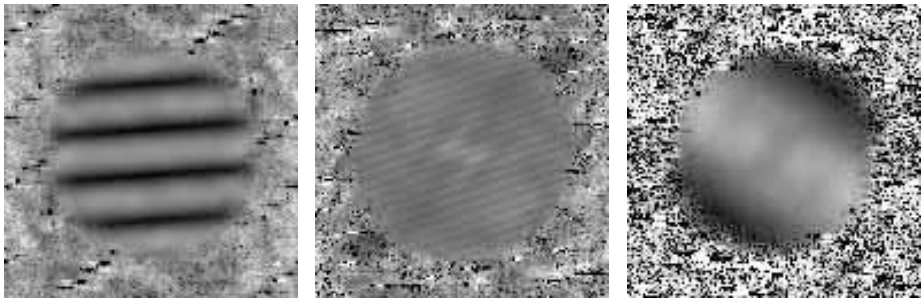

Figure 2. Examples of visibilities of binary stars (from Köhler et al. 2000). The star to the left is RX J1602.9-2022, the same as in Fig. 1. It has a separation of $0.31''$, a position angle of $5.3°$, and a flux ratio of 0.85. The binary in the middle panel is RX J1544.0-3311. Its parameters are $1.4''$, $200°$, and 0.07. The one to the right is RX J1604.3-2130B. It has $0.08''$, $327°$, and 0.7, so its separation is about half the diffraction limit of the telescope used ($\lambda/D = 0.13''$). The visibility is limited to a circular region because of the diffraction limit of the telescope. We cannot recover structures at frequencies higher than the cut-off, thus we see only noise there.

4. Reconstructing the Phase

The visibility of an object is always symmetrical, even if the object is not (e.g. in a binary with components of different brightness, cf. Fig. 2). Thus, we can measure the position angle only with a $180°$ ambiguity. To overcome this limitation, we need the full complex visibility, modulus and phase.

A method to reconstruct the phase of the complex visibility was proposed by Knox & Thompson (1974). This method uses the cross-spectrum of the image, i.e. the product of two different points in frequency space:

$$\begin{aligned} < \tilde{I}(u)\,\tilde{I}^*(v) > &= |\tilde{I}(u)|\,e^{i\varphi(u)} \cdot |\tilde{I}(v)|\,e^{-i\varphi(v)} \\ &= |\tilde{I}(u)|\,|\tilde{I}(v)|\,e^{i(\varphi_{\rm obj}(u)-\varphi_{\rm obj}(v)+\varphi_{\rm PSF}(u)-\varphi_{\rm PSF}(v))}\,, \end{aligned}$$

where $\varphi_{\rm obj}$ is the true phase of the object, and $\varphi_{\rm PSF}$ are the distortions introduced by the atmosphere. For small differences in frequency $|u - v|$, the phase differences are constant over time, so we can use the reference star to get the phase difference of the distortions:

$$\varphi_{\rm PSF}(u) - \varphi_{\rm PSF}(v) = {\rm Phase}(< \tilde{I}_{\rm ref}(u)\,\tilde{I}^*_{\rm ref}(v) >)$$

and therefore

$$\varphi_{\rm obj}(u) - \varphi_{\rm obj}(v) = {\rm Phase}(< \tilde{I}_{\rm obj}(u)\,\tilde{I}^*_{\rm obj}(v) >) - {\rm Phase}(< \tilde{I}_{\rm ref}(u)\,\tilde{I}^*_{\rm ref}(v) >).$$

With these phase differences, we can iteratively reconstruct the phase at all frequencies, starting from frequency zero. Since the image is real, its Fourier

Figure 3. Phases reconstructed using the Knox-Thompson-method of the same binaries as in Fig. 2. The phase of a binary shows characteristic jumps at the position of the minima of the visibility.

transform at frequency zero (which is simply the integral over the image) is also real and its phase is therefore zero. The phase at frequency one is then derived from $< \tilde{I}(1)\,\tilde{I}^*(0) >$ and so on. Figure 3 shows the phases reconstructed this way for the same binaries as in Fig. 2.

Lohmann and Weigelt developed a different method to reconstruct the phase (Weigelt 1977, Lohmann et al. 1983), called speckle masking or bispectrum-method. The bispectrum is the product of three points in the Fourier-transformed image:

$$\tilde{B}(u,v) =< \tilde{I}(u)\,\tilde{I}(v)\,\tilde{I}^*(u+v) > .$$

The phase of this quantity is quite insensitive to atmospheric distortions, similar to the closure phase in long-baseline interferometry. This gives another way to compute the phase at frequency $u+v$:

$$\varphi(u+v) = \varphi(u) + \varphi(v) - \mathrm{Phase}(\tilde{B}(u,v)).$$

Similar to the Knox-Thompson-method, this relation can be used to reconstruct the phase iteratively, starting at frequency 0.

Figure 4 shows that we can indeed obtain images of binaries by Fourier-transforming visibility and phase. The components of the binaries with medium and large separations are clearly visible, but the close binary is hardly detectable in image space. In comparison, its extended nature is obvious in the visibility in Fig. 2. This is one of the reasons why we hardly ever compute the back-transform, but fit binary models to the complex visibility in Fourier space.

5. Hardware

Speckle interferometry requires a camera for recording the data that has certain unusual properties. First of all, the pixel size has to be small enough to Nyquist-sample the diffraction limit of the telescope. This means that two pixels are the

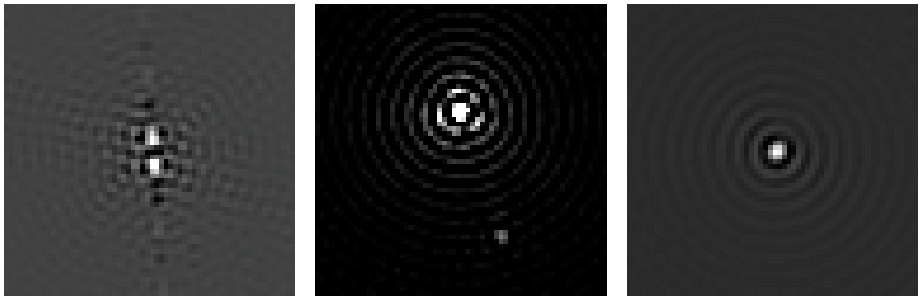

Figure 4. Images obtained by Fourier-transforming visibilities from Fig. 2 and phases from Fig. 3 back into image space.

size of a diffraction element λ/D, where λ is the wavelength and D the diameter of the telescope. For example, for observations in K-band at a 2-m telescope, the pixels should be smaller than about $0.1''$.

The second requirement is that it must be possible to take images with short exposure times, of the order of 0.1 seconds. This often implies that one either has to use a small detector, or one can only read out a subarray of a large detector. Therefore, the field-of-view of the images is usually limited. Fortunately, since we are interested in high spatial resolution, a field-of-view of 10 to 15 arcseconds is usually sufficient for the scientific program.

Third, we have to take a large number of images (several hundred to thousand). The electronics and the data storage behind the camera has to process the images at a rate comparable to the rate they are taken. This was quite demanding in the 1990s, but is not a problem with modern computers and hard disks.

A modern example of an instrument suitable for speckle interferometry is AstraLux at the 2.2 m telescope on Calar Alto (Hormuth et al. 2008.)[2]. The heart of AstraLux is the commercial camera DV887-UVB from Andor Technologies. The detector is sensitive at visual wavelengths between 400 nm and about 1000 nm. Since the coherence time of the atmosphere is longer for longer wavelengths, a filter is used that blocks light with wavelength shorter than 800 nm. The camera was designed for lucky imaging, but it is also possible to use the data for speckle interferometry. A sister instrument called AstraLux Sur was built for the New Technology Telescope at La Silla, Chile.

[2]see also `http://www.mpia-hd.mpg.de/ASTRALUX/`
or `http://www.caha.es/CAHA/Instruments/ASTRALUX/`

6. Scientific Examples

The "golden age" of speckle interferometry – at least in Germany – was in the 1990s. At that time, the first infrared detector arrays capable of short exposure times became available, while adaptive optics systems were not yet ready for routine observations.

Examples for science carried out with speckle interferometry are surveys for multiple stars in several star-forming regions (Taurus-Auriga: Leinert et al. 1993, Ghez et al. 1993, Köhler & Leinert 1998; several southern star-forming regions: Ghez et al. 1997; Scorpius-Centaurus: Köhler et al. 2000). The main result of these surveys was that most T Tauri stars form in binary or multiple systems. Speckle interferometry also allowed to resolve many of the high-mass stars in the Orion Nebular Cluster (Weigelt et al. 1999, Preibisch et al. 1999).

Follow-up observations of binaries discovered by speckle interferometry show in many cases orbital motion of the components. One example is the triple star LHS 1070, where the close pair has completed a full orbit since its discovery in 1993 (Fig. 5). About half of the orbit has been observed with speckle interferometry at 3.5 m telescopes. After the decommissioning of the speckle cameras in 2001, we continued to follow the orbit with the adaptive optics system NACO at the 8 m Very Large Telescope.

LHS 1070 is a favourable case because of its small distance of less than 8 pc. In Taurus-Auriga at about 140 pc distance, a binary with a projected separation of 0.13″ will have an orbital period of at least 80 years. However, such a binary has completed a significant fraction of its orbit since its discovery in 1990 – 1992. We are monitoring several close binaries and will soon present preliminary orbit solutions.

7. Conclusions

Speckle interferometry is a well-proven technique for the study of binary stars. Observations routinely reach the diffraction limit of the telescope and it is possible to detect binaries with even smaller separations. The hardware requirements are modest by today's standards, which makes it one of the best methods for diffraction-limited imaging at small telescopes.

Speckle interferometry also has some disadvantages: it is only possible to observe bright sources (brighter than ~ 10 mag in the K-band) with a relatively small dynamic range ($\Delta K \lesssim 3$ mag). The field-of-view is limited to the region where the PSF is constant (the isoplanatic patch, diameter $\sim 40''$). In practice, the method is limited by the size of detector arrays that can be read out fast enough, which allows to cover only about 15″. Nevertheless, there are plenty of binaries that can be observed.

Acknowledgements. I thank the organizers for inviting me to this interesting workshop.

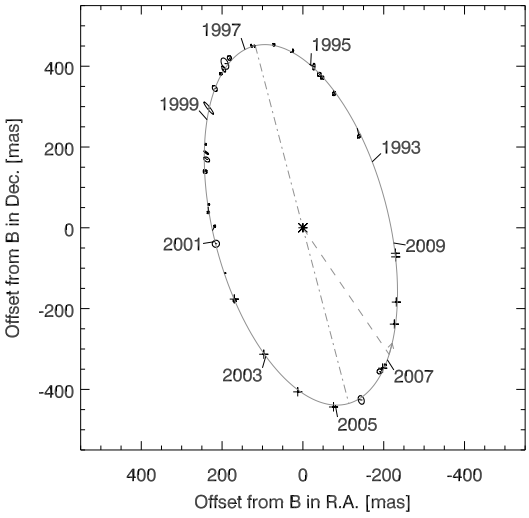

Figure 5. The orbit of components B and C in the triple system LHS 1070. Data points obtained with speckle interferometry are marked by their error ellipses, while crosses indicate measurements with adaptive optics (from Köhler et al. 2012).

References

Ghez, A. M., Neugebauer, G., Matthews, K.: 1993, *Astron. J.* **106**, 2005

Ghez, A. M., McCarthy, D. W., Patience, J. L., Beck, T. L.: 1997, *Astrophys. J.* **481**, 378

Hormuth, F., Hippler, S., Brandner, W., Wagner, K., Henning, T.: 2008, *Proceedings of the SPIE* **7014**, 701448

Köhler, R., Leinert, Ch.: 1998, *Astron. Astrophys.* **331**, 977

Köhler, R., Kunkel, M., Leinert, Ch., Zinnecker, H.: 2000, *Astron. Astrophys.* **356**, 541

Köhler, R., Ratzka, T., Leinert, Ch.: 2012, *Astron. Astrophys.* **541**, A29

Knox, K. T., Thompson, B. J.: 1974, *Astrophys. J.* **193**, L45

Labeyrie, A.: 1970, *Astron. Astrophys.* **6**, 85

Leinert, Ch., Zinnecker, H., Weitzel, N., Christou, J., Ridgway, S. T., Jameson, R., Haas, M., Lenzen, R.: 1993, *Astron. Astrophys.* **278**, 129

Leinert, Ch.: 1994, in *Star Formation and Techniques in Infrared and mm-Wave Astronomy*, eds.: T. P. Ray and S. V. W. Beckwith, Springer, Berlin, 215

Lohmann, A. W., Weigelt, G., Wirnitzer, B.: 1983, *Applied Optics* **22**, 4028

Preibisch, T., Balega, Y., Hofmann, K.-H., Weigelt, G., Zinnecker, H.: 1999, *New Astronomy* **4**, 531

Weigelt, G. P.: 1977, *Optics Communications* **21**, 55

Weigelt, G., Balega, Y., Preibisch, T., Schertl, D., Schöller, M., Zinnecker, H.: 1999, *Astron. Astrophys.* **347**, L15